A SIMPLE ALGORITHM FOR IDENTIFYING PERIODS OF SNOW ACCUMULATION ON A RADIOMETER

Karl E. Lapo[1], Laura M. Hinkelman[2], Christopher C. Landry[3], Adam K. Massmann [4], and Jessica D. Lundquist[5]

ABSTRACT

Downwelling solar, Q_{si}, and longwave, Q_{li}, irradiances at the earth's surface are the primary energy inputs for many hydrologic processes, and uncertainties in measurements of these two terms confound evaluations of estimated irradiances and negatively impact hydrologic modeling. Observations of Q_{si} and Q_{li} in cold environments are subject to conditions that create additional uncertainties not encountered in other climates, specifically the accumulation of snow on uplooking radiometers. To address this issue, we present an automated method for estimating these periods of snow accumulation. Our method is based on forest interception of snow and uses common meteorological observations. In this algorithm, snow accumulation must exceed a threshold to obscure the sensor and is only removed through scouring by wind or melting. The algorithm is evaluated at two sites representing different mountain climates: 1) Snoqualmie Pass, Washington (maritime) and 2) the Senator Beck Basin Study Area, Colorado (continental). The algorithm agrees well with time-lapse camera observations at the Washington site and with multiple measurements at the Colorado site, with 70 to 80% of observed snow accumulation events correctly identified. We suggest using the method for quality controlling irradiance observations in snow-dominated climates where regular, daily maintenance is not possible. Code for running the quality control algorithm can be found at https://github.com/klapo/moq. (KEYWORDS: solar irradiance, radiometer, interception, Senator Beck Basin, Colorado)

INTRODUCTION

The solar irradiance incident on the earth's surface (Q_{si}) is the primary energy input for many processes of interest in hydrology, in particular snow melt (Cline, 1997) and evapotranspiration (Gong et al., 2006; Xu et al., 2006). Uncertainties in observations of Q_{si} can directly impact studies and applications that utilize these data, for example, simulating melt in both physically-based (Lapo et al., 2015) and index snow models (Slater et al., 2013). Mizukami et al. (2014) found that differences between estimated Q_{si} datasets used to force a hydrologic simulation of the upper Colorado River basin led to a 20% difference in simulated run-off at high elevations, and both they and Xia et al. (2005) found that uncertainty in Q_{si} adversely affected model calibration. Additionally, well-known but poorly-documented observational uncertainties have hindered development of estimated and modeled irradiances in the past (Philipona, 2002). Lundquist et al., (2015) argue that "insidious" observational errors, those that are difficult to identify through traditional methods, impede model development and process understanding, and recommend improved quality control techniques as part of reducing and recognizing observational uncertainties. In this paper we describe a strategy for reducing a potentially large source of uncertainty in observations of Q_{si}.

Conditions in cold regions create observational problems not encountered in other climates--observation sites are often located in rugged and remote locations that make regular maintenance difficult. Previous studies have noted that radiometers in cold environments can become obscured as snow accumulates on the uplooking sensor (Figure 1) and can cause erroneously low downwelling shortwave and high downwelling longwave values (Malek, 2008; Landry et al., 2014). In this note, we focus on the accumulation of snow on uplooking pyranometers and pyrgeometers. We refer to these events as snow-on-dome events (SOD), but they can include instances where snow accumulates around the aperture of the instrument, on the body of the radiometer, which still affects the sky view of the instrument.

There are several strategies currently employed for accounting for SOD. At the highest quality sites, regular, daily (or more frequent) maintenance removes snow (World Meteorological Organization, 2008). Malek et

Paper presented Western Snow Conference 2015
[1] Karl Lapo, Atmospheric Sciences, University of Washington, Seattle, WA, lapok@uw.edu
[2] Laura M. Hinkelman, Joint Institute for the Study of the Atmosphere and Ocean, Seattle, WA, laurahin@uw.edu
[3] Christopher C. Landry, Center for Snow and Avalanche Studies, Silverton, Colorado, clandry@snowstudies.org
[4] Adam K. Massmann, Dept. of Atmos. & Env'tl Sciences, Univ. at Albany, Albany, NY, amassmann@albany.edu
[5] Jessica D. Lundquist, Civil and Env. Engineering, University of Washington, Seattle, WA, jdlund@uw.edu

al. (2008) suggest that SOD can be avoided with ventilated radiometers. These solutions are not feasible at many observation sites due to limited accessibility and power supply. Additionally, ventilated radiometers may not be effective at removing snow under some conditions, for instance wet, heavy snow commonly found in maritime climates (Figure 1). Other methods of burial detection rely on rare measurements, like reflected shortwave (Raleigh, 2013), or regular, daily maintenance (World Meteorological Organization, 2008). The snow burial algorithm is an easily implemented method for reducing this uncertainty, especially when these other methods are not available.

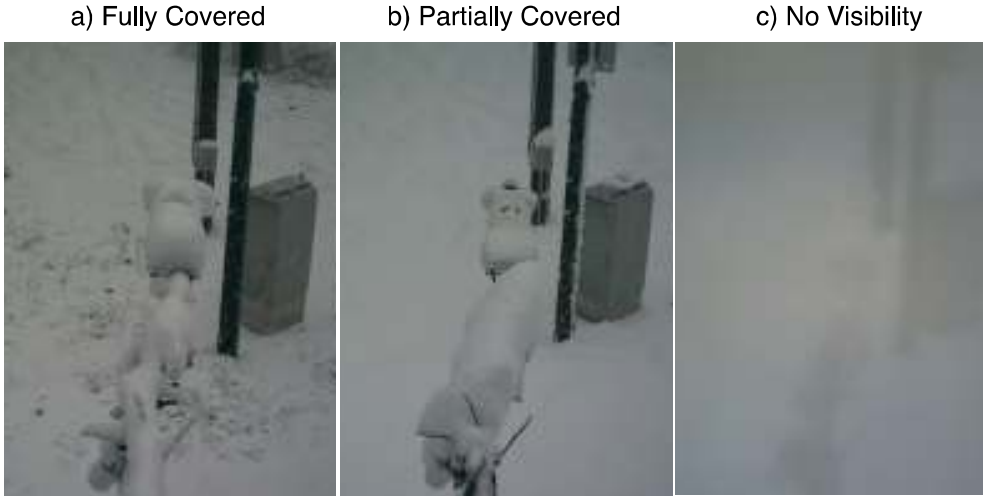

Figure 1. Time lapse photos of the ventilated 4-stream radiometer at Snoqualmie Pass demonstrating different SOD classification used in the algorithm evaluation.

SNOW ON DOME ALGORITHM

Snow on dome (SOD) events are detected using a simple algorithm that uses co-observed precipitation, air temperature, and wind speed. Effectively, the algorithm approximates a radiometer as a tree branch that is intercepting snow; if a branch is intercepting snow, the radiometer is likely to be intercepting snow also. The SOD algorithm has tunable parameters for which values were determined from studies of tree interception (Table 1). In using interception studies for developing the SOD algorithm, our goal is to create a robust method that is not dependent on parameter tuning at a limited number sites and therefore applicable to a variety of climates. The algorithm is outlined in Figure 2.

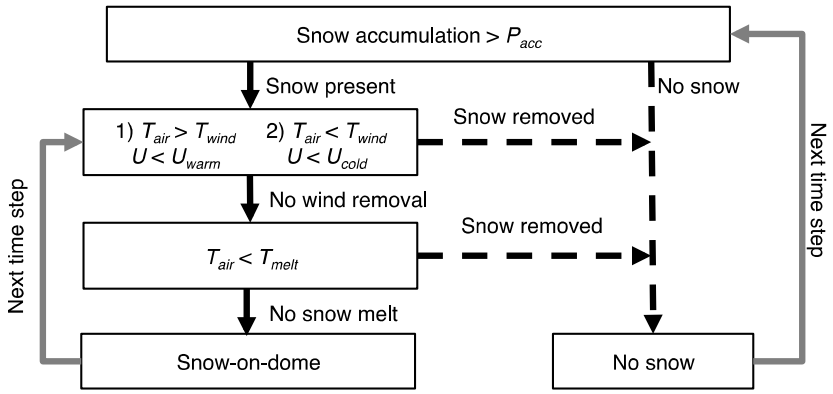

Figure 2. Flow chart of the snow detection algorithm. T_{melt} is the threshold for melting snow off the radiometer, T_{wind} is the threshold between "warm" and "cold" wind removal, determined by the U_{warm} and U_{cold} wind thresholds, and P_{acc} is the rate of snow water equivalent accumulation before the algorithm triggers SOD.

DATA

Snoqualmie Pass (SNQ)

Snoqualmie Pass (SNQ), Washington has a maritime climate and is located in the rain-snow transition zone (917 m). Observations include: precipitation, air temperature, wind, relative humidity, surface temperature, incoming and outgoing longwave irradiance, and incoming and reflected shortwave irradiance (Lundquist et al., 2014).

Senator Beck Basin Study Area (SBBSA)

SBBSA, in the Red Mountain Creek catchment of the western San Juan Mountains of Colorado, includes two study plots, the Swamp Angel Study Plot (SASP, 3371 m) and the Senator Beck Study Plot (SBSP, 3714 m), which each observe air temperature, wind, relative humidity, surface temperature, incoming longwave irradiance, and incoming and reflected shortwave irradiance. SBSP is located above the tree line in an alpine meadow. No precipitation observations are made at SBSP, as snow accumulation is strongly influenced by wind. SASP, 1.3km away, is a sub-alpine site located within a large forest clearing. Precipitation is measured at this site due to the consistently lower wind speeds. These lower wind speeds also allow snow to accumulate on the uplooking radiometers, a problem that does not occur as often at the more exposed SBSP (Landry et al., 2014).

Identifying Periods with Snow on the Radiometer

In both study areas we employed additional observations, not typically made, in order to derive an independent record of SOD events. At SNQ, we took advantage of a time-lapse camera located on the tower that directly over looked the radiometer (water year 2014, Figure 1). Photos were taken at an hourly interval in water year 2014. At SNQ we directly observed SOD events during daytime using these time-lapse photographs. Every photograph was visually classified as snow-free, fully-covered by snow (one or both of the pyranometer and pyrgeometer domes completely covered by snow, Figure 1a), partially covered by snow (including snow on the body of the radiometers, Figure 1b), or no visibility due to fog or camera failure (Figure 1c). Both partially- and fully-covered designations are interpreted to indicate SOD in the algorithm evaluation.

At SASP and SBSP we took advantage of the site pairing, where one site is regularly snow free (SBSP) when the instruments at the other are covered by snow (SASP). We assume the pyranometer and pyrgeometer at one location will be covered simultaneously and can infer snow presence on SASP instruments using observations from both sites that meet the following requirements simultaneously: (1) The observed downwelling longwave irradiance and the longwave irradiance for a blackbody emitting at the local air temperature are within 5%; in conjunction with either: (2a) Q_{si} observed at SASP is less than 90% of the value observed at SBSP or (2b) the derived albedo at SASP is greater than 0.9. This method of SOD detection is referred to as the "inferred snow" method. Regular maintenance is performed at the SBBSA stations, including brushing snow off the radiometers. The inferred snow method correctly identified 76% of SOD events according to the maintenance logs. Errors resulted in cases when the pyranometer was snow covered but the pyrgeometer was not, or when the pyranometer at SASP was snow covered but SASP Q_{si} was enhanced relative to observations at SBSP, perhaps due to reflections from the snow surrounding the dome.

ALGORITHM PERFORMANCE

Evaluation

The algorithm was independently verified at SNQ in water year 2014 using the time-lapse camera (e.g. Figure 3) and SASP during water years 2011 and 2012 using the inferred snow method. The SOD algorithm and time-lapse camera classifications compare well for an example storm at SNQ in water year 2014 (Figure 3). Small amounts of snow fell at the beginning of this example period (February 7th-8th), triggering the SOD algorithm. However, the time-lapse camera and algorithm disagreed on the duration of this event, as higher winds led to snow removal in the SOD algorithm. From the 9th onward, significant amounts of snow fell, covering the radiometers, leading to low Q_{si} and high Q_{li} observed values. The algorithm and time-lapse camera effectively agreed on the timing of snow removal from the radiometers, during the night between the 10th and the 11th.

We evaluate the algorithm's performance using the Gilbert Skill Score (GSS), probability of detection (POD), and false alarm ratio (FAR) (Hogan et al., 2010) (Table 2). GSS measures the fraction of events that are correctly predicted after taking into account the random chance of a yes event, based on the observed frequency; a negative GSS means no skill, a GSS equal to zero is the expected value of a random prediction, and any GSS greater than 0, up to a value of 1, indicates a prediction method with increasing skill. The GSS allows a comparison across climates with differing frequency of events. We also include POD, which tells us the fraction of observed SOD events that were predicted using the algorithm and FAR, which tells us the fraction of SOD events predicted in the algorithm that did not occur.

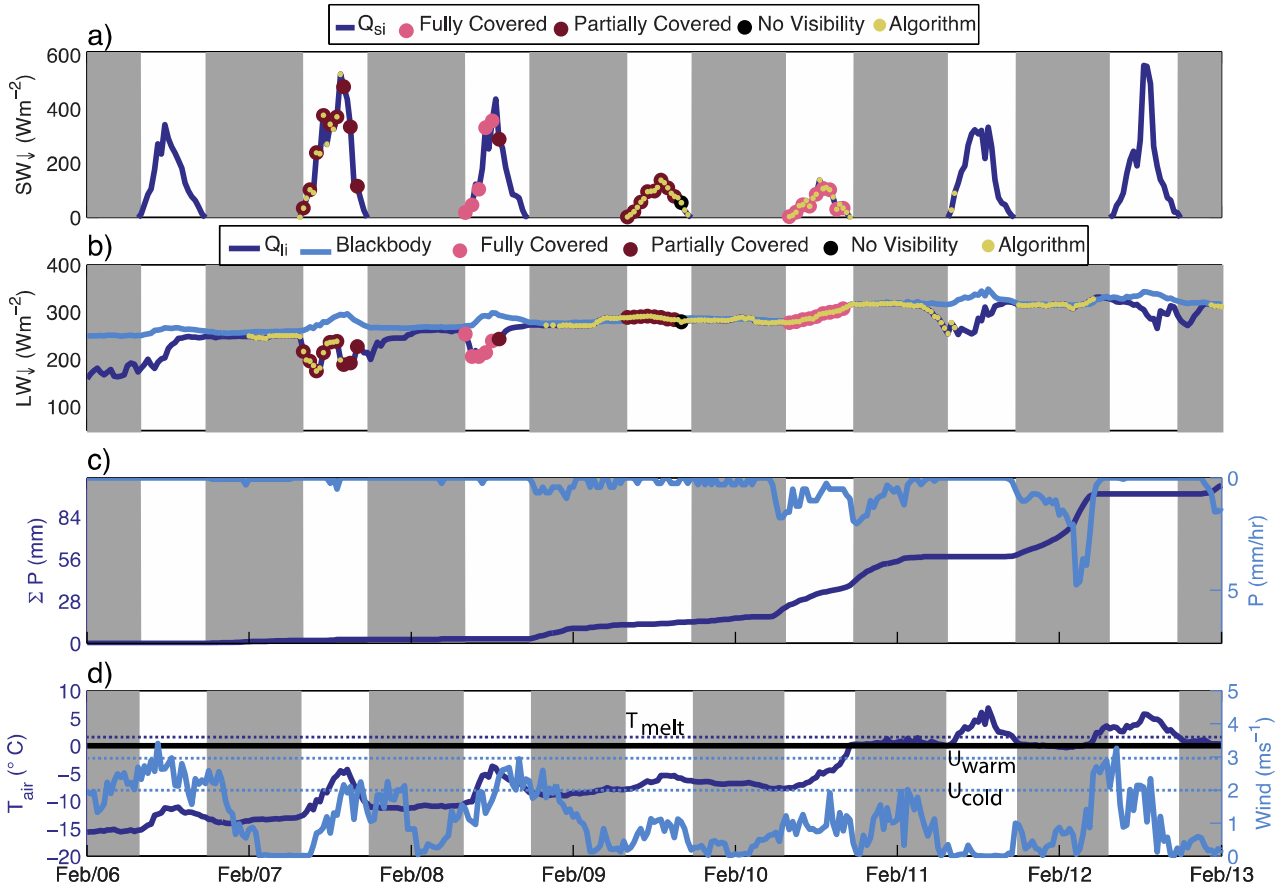

Figure 3. Example of the SOD algorithm classification (yellow dots) during a storm at SNQ in water year 2014. Nighttime is shown with grey bars. a) Q_{si} observations, with time-lapse classifications (Figure 1) b) Q_{li} observations and the irradiance from a blackbody emitting at the observed air temperature. The time lapse classifications (pink, red, and black dots, see Figure 1) are also shown. c) Accumulated and rate of precipitation. d) Air temperature and wind speed with labeled removal thresholds (Figure 2).

The algorithm evaluates well as measured by POD and is able to detect most SOD events (approximately 70% to 80%). The algorithm does produce a fairly high FAR (between 29% and 43%). Thus, it flags more data as suspect than allows suspect data through. The high false alarm ratio also explains the lower GSS given the high POD. Performance was similar in the two different climates (maritime and continental), suggesting that the algorithm for detecting SOD events is robust in regards to climate.

Table 1. Evaluation statistics for the algorithm at both sites. We treat snow detection as a binary event and thus employ evaluation from a contingency table.

Site	Water Year	Gilbert Score	False Alarm Ratio	Probability of Detection
SNQ	2014	0.46	0.43	0.77
SASP	2011	0.57	0.29	0.83
SASP	2012	0.56	0.34	0.85

Algorithm Impact

To briefly examine how the frequency of SOD varies significantly depending on site climate and conditions, the SOD algorithm was run at 9 AmeriFlux sites and 7 snow study sites (Table 3). This analysis is meant as a quick demonstration of the applicability of the algorithm and how local conditions impact the occurrence of SOD in the absence of maintenance, not as a thorough quality control of the data from these sites. The AmeriFlux network installs pyranometers above the canopy, leading to overall higher winds. This particular site set-up likely explains the lower frequency of estimated SOD frequency. In contrast, typical snow study sites (i.e., SASP, SNQ, Reynolds Mountain Sheltered Site, and Dana Meadows) are located below canopy in clearings where wind speeds are typically lower, allowing SOD to occur much more frequently. The characteristics of these sites are typical of sites designed for observing precipitation (sheltered in a forest clearing, below canopy) and are also the characteristics that make these sites most susceptible to SOD. More exposed sites (SBSP and Reynolds Mountain Exposed Site) show similar snow on dome frequencies as observations made above canopy, but are not typical of snow study sites keyed for observing precipitation.

Site	Time SOD estimated (%, annual)	Time SOD estimated (%, DJF)	Network
Flagstaff Managed Forest, AZ	0.4	1.1	AmeriFlux
Glacier Lakes Ecosystem Experiments Site, WY	1.0	1.2	AmeriFlux
Metolius Second Young Pine, OR	2.4	8.4	AmeriFlux
Valles Caldera Ponderosa Pine, AZ	7.2	18.7	AmeriFlux
Niwot Ridge, CO	3.9	4.5	AmeriFlux
Dana Meadows, CA	10.0	22.3	California Dept. Water Res.
Reynolds Mountain Exposed Site, ID	1.1	1.6	(Reba et al., 2011)
Reynolds Mountain Sheltered Site, ID	12.7	25.9	(Reba et al., 2011)
Senator Beck, CO	13.4	18.7	(Landry et al., 2014)
Swamp Angel, CO	30.0	59.2	(Landry et al., 2014)
Snoqualmie, WA	20.7	38.5	(Lundquist et al., 2014)

Table 2. Percent of time steps in which the algorithm estimates snow on the pyranometer (in the absence of maintenance) at sites from the AmeriFlux network, along with typical snow observation sites.

CONCLUSION

Radiometers left untended in snowy environments, which generally have harsh conditions and difficult access, are subject to conditions that increase the uncertainty in their observed values, with implications for a wide range of hydrology studies. Snow accumulating on or around a radiometer will lead to erroneous observations. While this problem is likely known among most site operators, the detection and flagging of these events is not standard. In the past, these sorts of observational uncertainties have hindered development of estimated and modeled irradiances. The SOD algorithm is an easily implemented method for reducing this uncertainty, especially when other methods are not available. For this reason, we recommend that it should be employed for quality control purposes at sites that are unable to meet WMO standards for sensor maintenance.

REFERENCES

Cline, D. W. 1997. Snow surface energy exchanges and snowmelt at a continental, midlatitude Alpine site, *Water Resour. Res.*, *33*(4), 689–701.

Gong, L., C. Y. Xu, D. Chen, S. Halldin, and Y. D. Chen. 2006, Sensitivity of the Penman-Monteith reference evapotranspiration to key climatic variables in the Changjiang (Yangtze River) basin, *J. Hydrol.*, *329*(3-4), 620–629, doi:10.1016/j.jhydrol.2006.03.027.

Hogan, R. J., C. a. T. Ferro, I. T. Jolliffe, and D. B. Stephenson. 2010, Equitability Revisited: Why the "Equitable Threat Score" Is Not Equitable, *Weather Forecast.*, *25*(2), 710–726, doi:10.1175/2009WAF2222350.1.

Landry, C. C., K. A. Buck, M. S. Raleigh, and M. P. Clark. 2014. Mountain system monitoring at Senator Beck Basin, San Juan Mountains, Colorado: A new integrative data source to develop and evaluate models of snow and hydrologic processes, *Water Resour. Res.*, *50*, 1–16, doi:10.1002/2013WR013711.Received.

Lapo, K. E., L. M. Hinkelman, M. S. Raleigh, and J. D. Lundquist. 2015. Impact of errors in the downwelling irradiances on simulations of snow water equivalent, snow surface temperature, and the snow energy balance, *Water Resour. Res.*, *50*, n/a–n/a, doi:10.1002/2014WR016259.

Lundquist, J. D., A. K. Massman, J. Stimberis, and N. E. Wayand. 2014. *Surface Meteorological and Snow Observations at Snoqualmie Pass, WA*, Seattle, WA.

Lundquist, J. D., N. E. Wayand, A. K. Massman, M. P. Clark, F. Lott, and N. C. Cristea. 2015. Diagnosis of insidious data disasters, *Water Resour. Res.*, *51*, doi:10.1002/2014WR016585.

Malek, E. 2008. The daily and annual effects of dew, frost, and snow on a non-ventilated net radiometer, *Atmos. Res.*, *89*(3), 243–251, doi:10.1016/j.atmosres.2008.02.006.

Mizukami, N., M. P. Clark, A. G. Slater, L. D. Brekke, M. M. Elsner, J. R. Arnold, and S. Gangopadhyay. 2014. Hydrologic Implications of Different Large-Scale Meteorological Model Forcing Datasets in Mountainous Regions, *J. Hydrometeorol.*, *15*(1), 474–488, doi:10.1175/JHM-D-13-036.1.

Philipona, R. 2002. Underestimation of solar global and diffuse radiation measured at Earth's surface, *J. Geophys. Res.*, *107*(D22), 4654, doi:10.1029/2002JD002396.

Raleigh, M. S. 2013. Quantification of Uncertainties in Snow Accumulation, Snowmelt, and Snow Disapperance Dates, University of Washington, Seattle, Washington, United States.

Reba, M. L., D. Marks, M. Seyfried, A. Winstral, M. Kumar, and G. N. Flerchinger. 2011. A long-term data set for hydrologic modeling in a snow-dominated mountain catchment, *Water Resour. Res.*, *47*(7), 1–7, doi:10.1029/2010WR010030.

Slater, A. G., A. P. Barrett, M. P. Clark, J. D. Lundquist, and M. Raleigh. 2013. Uncertainty in seasonal snow reconstruction: Relative impacts of model forcing and image availability, *Adv. Water Resour.*, *55*, 165–177.

World Meteorological Organization. 2008. Measurement of radiation, in *Guide to Meteorological Instruments and Methods of Observation*, pp. I.7–1–1.7–42, World Meteorological Organization, Geneva, Switzerland.

Xia, Y., Z.-L. Yang, P. L. Stoffa, and K. Sen Mrinal. 2005. Using different hydrological variables to assess the impacts of atmospheric forcing errors on optimization and uncertainty analysis of the CHASM surface model at a cold catchment, *J. Geophys. Res.*, *110*(D1), 1–15, doi:10.1029/2004JD005130.

Xu, C. Y., L. Gong, T. Jiang, D. Chen, and V. P. Singh. 2006. Analysis of spatial distribution and temporal trend of reference evapotranspiration and pan evaporation in Changjiang (Yangtze River) catchment, *J. Hydrol.*, *327*(1-2), 81–93, doi:10.1016/j.jhydrol.2005.11.029.